Journal of Maps

ISSN: (Print) (Online) Journal homepage: https://www.tandfonline.com/loi/tjom20

UAV and field survey observations on the November 26th 2022 Celario flowslide, Ischia Island (Southern Italy)

Melania De Falco, Giovanni Forte, Ermanno Marino, Luigi Massaro & Antonio Santo

To cite this article: Melania De Falco, Giovanni Forte, Ermanno Marino, Luigi Massaro & Antonio Santo (2023) UAV and field survey observations on the November 26th 2022 Celario flowslide, Ischia Island (Southern Italy), Journal of Maps, 19:1, 2261484, DOI: 10.1080/17445647.2023.2261484

To link to this article: https://doi.org/10.1080/17445647.2023.2261484

JOURNAL OF MAPS
2023, VOL. 19, NO. 1, 2261484
https://doi.org/10.1080/17445647.2023.2261484

UAV and field survey observations on the November 26th 2022 Celario flowslide, Ischia Island (Southern Italy)

Melania De Falco[a], Giovanni Forte[a], Ermanno Marino[a], Luigi Massaro [a,b] and Antonio Santo[a]

[a]Department of Civil, Architectural and Environmental Engineering, Università degli Studi di Napoli Federico II, Naples, Italy; [b]Department of Earth Sciences, Royal Holloway University of London, Egham, United Kingdom

ABSTRACT

On 26th November 2022, a heavy cloudburst affected Ischia Island (Southern Italy) causing a flash flood and triggering several flowslides. The most affected municipality was Casamicciola Terme, where this event produced 12 casualties, more than 200 people evacuated and several damages to the buildings and the road network. The largest flowslide involved Celario watershed, which started as a small slide (around 10 m^3) on the top of Mt. Epomeo at 703 m a.s.l. of height and impacted downward at 645 m a.s.l., successively channelising in the catchment. This study summarises the geological and geomorphological evidence collected during the field investigation of the Celario flowslide and analyses the remotely sensed UAV data to reconstruct the occurred scenario. Finally, some considerations on the relationships between the occurred damage and the flowslide impact are discussed.

ARTICLE HISTORY
Received 17 May 2023
Revised 29 August 2023
Accepted 14 September 2023

KEYWORDS
Flowslide; UAV; weather-induced landslides; Ischia Island

1. Introduction

In the last decades, the impact of climate change is always more testified by the increase in the frequency of destructive rainfall-induced phenomena. This trend was observed in the study carried out by Neumayer and Barthel (2011), who analysed a dataset of weather-related disasters between 1980 and 2009. Between 2002 and 2014, Messeri et al. (2015) recorded 293 deaths in Italy and in 2013, the occurrence of 351 landslide and flood events. Similar data are also gathered in the 'Polaris' database (https://polaris.irpi.cnr.it) of the CNR IRPI, which collects information on the geo-hydrological risk in Italy since 1963 (Salvati et al., 2016). The frequency of natural hazards has been increasing in the last decades in Europe, and more specifically in the Mediterranean regions, due to climate change (Alvioli et al., 2018). In addition, the risk of natural disasters in Italy is still rising due to the increased population density, progressive urbanisation, abandonment of mountainous areas, unauthorised buildings, ongoing deforestation, and lack of maintenance of the slopes and channels. Santangelo et al. (2021) collected a dataset of debris flows events for the Campania region (southern Italy) highlighting a reduction in the years with no recorded flowslide events that passed from 18 years (1942–1959) to 12 years (1974–1985), 8 years (1988–1995), and only 4 years (2000–2003). In the period 2004–2019, the frequency increased to nearly one event per year. On the contrary, records of flash floods between 1996 and 2020 resulted to be 28 in 24 years, namely more than one event per year.

The most recent weather-induced disaster in Campania occurred on 26th November 2022, when a cloudburst affected the volcanic island of Ischia (Southern Italy) triggering several flowslides and alluvial floods. The most affected area resulted to be the small village of Casamicciola Terme, where twelve people, including a newborn and two children, lost their life. Pictures from field surveys and video footage from social media showed buildings smashed by the landslide and several cars and buses transported into the sea. The disaster was exacerbated by the presence of houses in high-risk areas at the foothill of Mt. Epomeo.

The Island is one of the most critical areas of Campania region, in fact in the last 113 years there have been 42 casualties by floods and landslides in different municipalities, as summarised in Table 1.

Furthermore, the Mw 3.9 earthquake that occurred in 2017 also contributed to the damage toll around Casamicciola and Lacco Ameno with 2 deaths, 42 injured and more than 2500 displaced people (Gargiulo et al., 2022).

In this work, the data collected following 26th November 2022 rainfall event are reported and summarised in order to describe the occurred scenario. Such case study is of interest to the international

CONTACT Luigi Massaro luigi.massaro@unina.it Università degli Studi di Napoli Federico II via Claudio 21, 80125, Napoli
Supplemental map for this article is available online at https://doi.org/10.1080/17445647.2023.2261484.

Table 1. Summary of the weather-induced events that affected Ischia Island in the last 113 years data from Del Prete and Mele (1999, 2006), Santo et al. (2012).

Date	Event	Location	Fatalities
24 October 1910	Flood and landslides	Casamicciola, Lacco Ameno	11, 4
3 October 1939	Rockfall	Casamicciola	1
18 February 1966	Landslide	Forio	1
7 June 1978	Rockfall	Barano d'Ischia	5
3 August 1983	Rockfall	Barano d'Ischia	1
23 March 1987	Landslide	Casamicciola	1
30 April 2006	Landslide	Ischia	4
10 November 2009	Flood	Casamicciola	1
25 February 2015	Landslide	Barano d'Ischia	1
26 November 2022	Flood and landslides	Casamicciola, Lacco Ameno	12

community because these hazardous phenomena occur worldwide where loose soils cover steep bedrocks threatening the communities living in the foothill area. The paper describes rainfall data (Section 2) and the geological setting (Section 3), afterward, it focuses on the methodology followed in the post-event survey (Section 4) for producing the Main Map. Finally, in Section 5, the lessons learned are summarised and commented in the conclusions.

2. The rainfall event occurred on 26th November 2022

On November 26th 2022, a heavy cloudburst caused an alluvial phenomenon (flash flood) and triggered several flowslides at Ischia Island, leading to 12 casualties, more than 200 people evacuated and several damages. In particular, the alluvial event developed from three sub-basins which have their closing section located upstream of Piazza Bagni in the centre of Casamicciola municipality. These three basins were already involved in the 2009 alluvial event (Santo et al., 2012). On 26th November 2022, they were reactivated and produced erosional phenomena along the hydrographic drainage network, with the transport of several cars and flooding of lower floors of the houses. Additionally, the area was also affected by several flowslides, the largest ones are three with extensions between 3000 and 70,000 m^2 and run-out distances between 300 and 1500 metres. In particular, Celario flowslide started as a small slide (around 10 m^3) on the top of Mt. Epomeo at 703 m a.s.l. and impacted downward at 645 m a.s.l. (as shown in the 'frontal orthomosaic of the crown area' in the Main Map). This small slide triggered the main flowslide, which increased its velocity and volume channelising in the Celario catchment and stopping after 1.5 km (see Figure 1 and the Main Map).

As regards the rainfalls, Ischia Island hosts four raingauges, namely Forio, Monte Epomeo, Piano Liguori and Ischia, whose locations are reported in Figure 2(a). In particular, the rainfall data recorded every 10 min between 26th and 27th November 2022 were collected for describing the occurred event as reported in Table 2. Additionally, they were also aggregated to estimate the accumulated and the maximum rainfall values at different durations. The data show the highest cumulative rainfall value (176.8 mm) recorded at the Forio raingauge, which can also be considered the most representative to analyse the ground effects in terms of distance from the event and elevation. The maximum rainfall value at 10 min was recorded for Monte Epomeo raingauge.

In Figure 2(b) the maximum hourly rainfall and the 3-month cumulated rainfall of the November 26th event were plotted in the classification diagram proposed by Santangelo et al. (2021). They identified two different fields of existence for Flash floods (FF) and Flowslides (FL) based on the difference in triggering rainfalls associated with the past events occurred in Campania. Flash floods are initiated by high daily/hourly rainfall values, while flowlides require high antecedent cumulative rainfall (e.g. 3 months before). The plot of the 26th November 2022 rainfall falls between the flowslides and flash floods boundary, which can be considered representative of the occurrence of both phenomena. Figure 2(c) shows the precipitation recorded every ten minutes at the Forio raingauge, where it is evident that the rainfall started at 24:00 and ended at 12:00 the next day. Furthermore, the highest values were measured between 04:00 and 06:00 reaching accumulated values of 79.6 mm in 2 h and 176.8 mm in 24 h. Additionally, considering the maximum rainfall at different durations of a 14-year time series, the 26th November 2022 rainfall can be considered exceptional as it shows higher values than the average and maximum values for the 1, 3, 6, 12 and 24-hour time intervals, as shown in Figure 2(d).

3. Geological and geomorphological setting

Ischia Island is part of a complex volcanic field, covering an area of about 42 km^2 in the north-western sector of the Gulf of Naples. Its geological and geomorphological setting is mainly characterised by steep volcanic lithologies and landforms, which determine a high susceptibility to instability events and processes. These include earthquakes, flowslides, rockfalls, flash floods, and tsunamis, defining an area prone to multi-hazard framework (Selva et al., 2019). The main lithologies outcropping are trachytes and latite-phonolites lava and pyroclastic soils and ancient mudflow deposits (Chiesa et al., 1987; Orsi et al., 1998).

The volcanic activity on Ischia Island is older than 150 ka, with five major phases recognised, up to the last event represented by the Arso eruption of 1302 (Chiesa et al., 1987; Civetta et al., 1991; Orsi et al., 1998). These eruptive phases are generally grouped

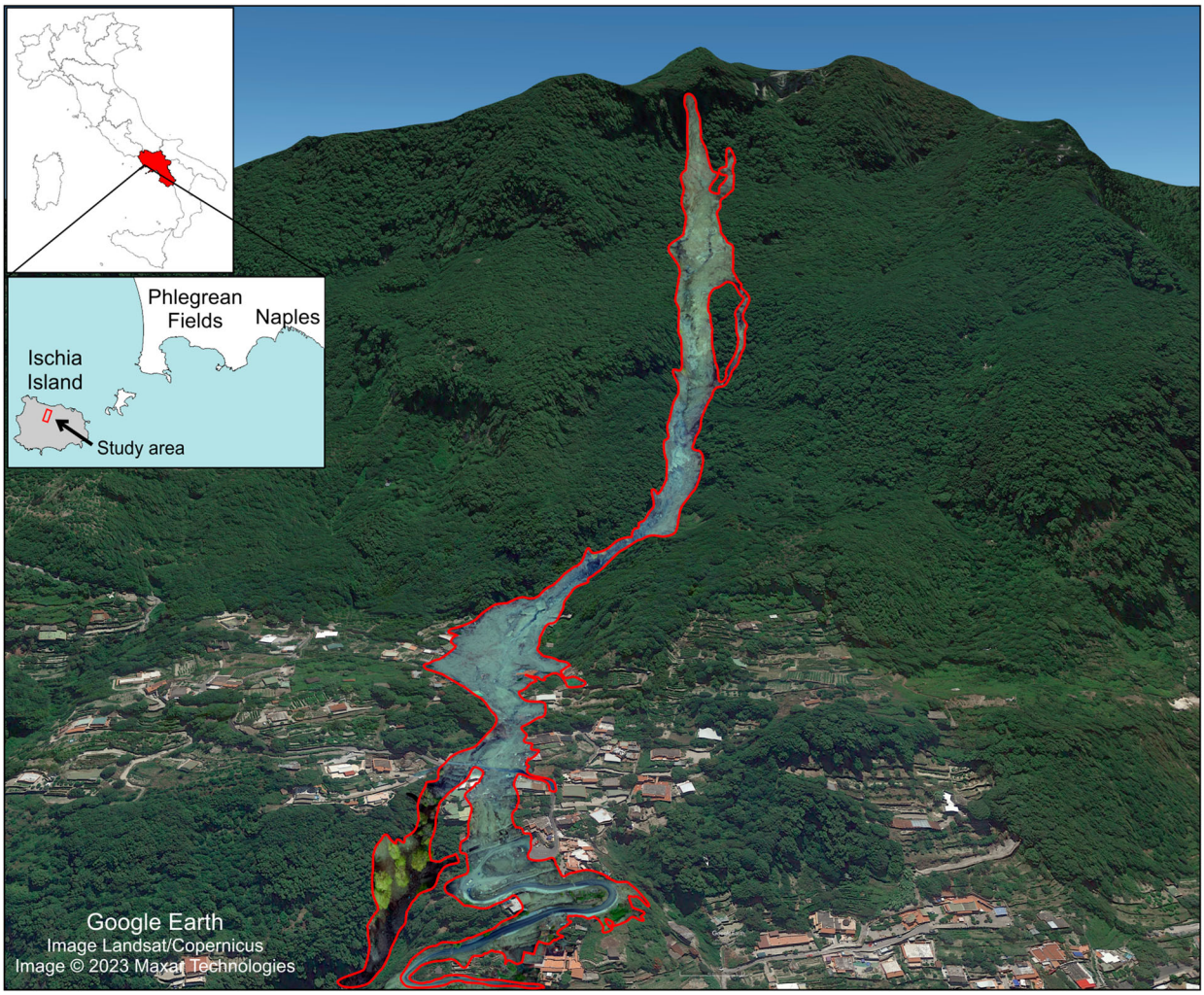

Figure 1. UAV-derived orthophoto of the Celario flowslide (red line) overlayed on the Google Earth satellite view.

into two main cycles, separated by a quiescent period of about 25 ka, and differentiated by the emplacement of the Green Tuff formation (about 55 ka). The latter constitutes the backbone of Mt. Epomeo and is a trachytic ignimbrite characterised by a green colour given by the alteration due to contact with seawater.

Casamicciola town is a residential, touristic and agricultural site lying at the base of the northern slope of Mt. Epomeo, which is a fault scarp characterised by high gradients. The steep walls of the main gullies and cliffs, especially along the coastal perimeter of the island, have repeatedly been affected by landslides and alluvial events (Del Prete & Mele, 1999, 2006).

4. Mapping methods

In this study, the Main Map includes a geological map with the landslide geological cross-section (Map 2), the geomorphological map (Map 3), a map estimating the thickness of erosion and deposition (Dem of Difference, DoD) with transversal topographic profiles (Map 4), and a map representing the building damage (Map 5). They were obtained by integrating classical field surveys with 3D reconstruction through SfM photogrammetry from UAV (Unmanned Aerial Vehicle) images acquired a week after the event (Map 1). The field survey was carried out for an area of about 0.5 km^2, it was aimed at documenting the triggering in the crown area, the evolution in terms of both erosion and accumulation, and assessing the damage in the urban area. The collected pictures and measurements were successively geolocated using the software Geosetter and waypoints taken with a GPS.

The photogrammetric survey was carried out with a high-performance drone (DJI Matrice 300 RTK) equipped with a high-resolution digital camera (DJI P1) making a flight at a constant height of 120 m above the ground over an area of about 0.5 km^2. The data acquisition was performed with a full-frame digital camera with a 45 megapixels sensor, producing a total of 844 pictures along a 3D flight plan. The UAV was supported by GNSS/RTK systems on board to obtain the precise absolute coordinate of each photo in its log file. The images have been acquired sequentially with an 80% side overlap and a GSD (ground sampling distance) of 2 cm. Automatic procedures have been done both for the orientation of the images and the 3D reconstruction using a

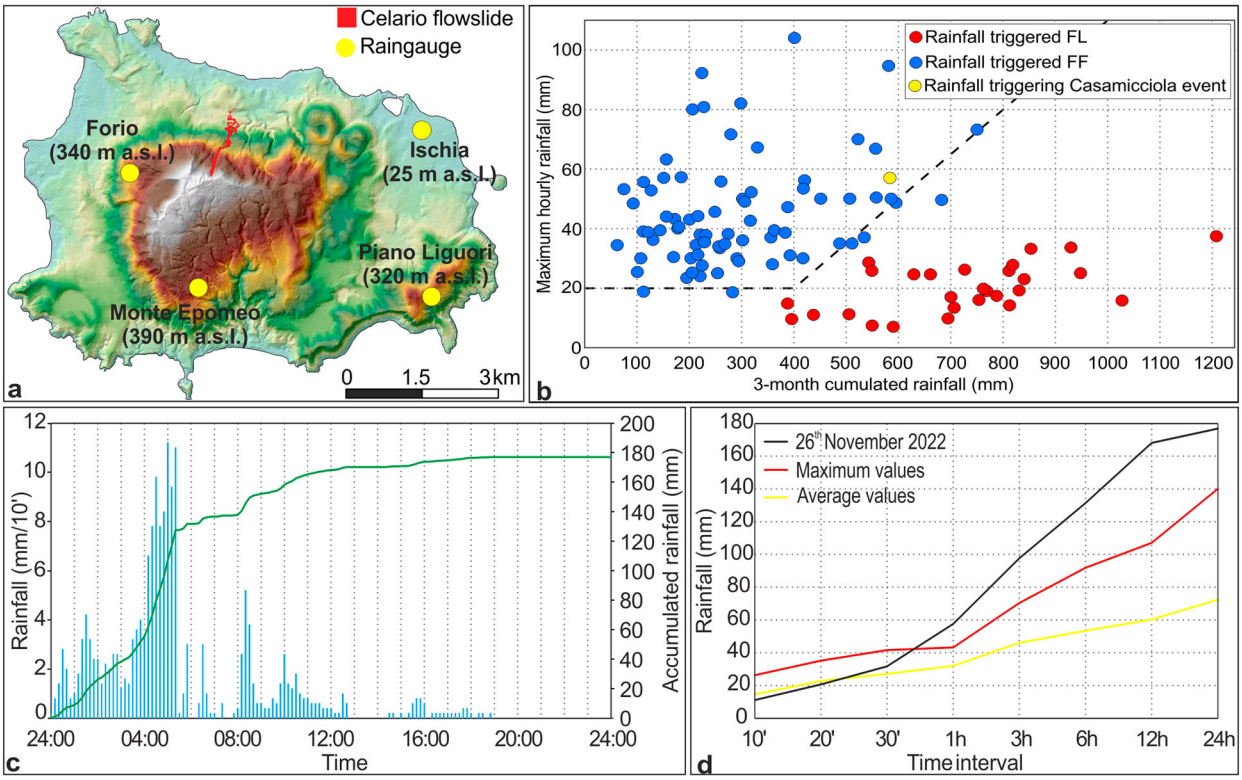

Figure 2. (a) Distribution of raingauges on Ischia Island. (b) Comparison of the 26th November rainfall values in the plot by Santangelo et al. (2021); (c) ten minutes recorded rainfall and cumulative value of the Forio raingauge; (d) Comparison of event values with the maximum and average rainfall at different duration in a 14-year time series.

bundle adjustment algorithm. Data processing allowed the development of an orthomosaic of the landslide area with a resolution of 2 cm and the digital elevation model (DEM) with a cell size of 3.30 cm. The latter was resampled with a 1 m cell size and compared with the DEM prior to the event. The latter was derived from a 2009 to 2012 LiDAR survey (1 × 1 m) provided by the Italian Ministry of the Environment. The DEMs comparison was performed with a DoD approach, which highlighted the most relevant topographic changes in terms of eroded and accumulated areas.

4.1. Map 1 – UAV orthomosaic and frontal view of the crown

The photogrammetric data processing allowed obtaining high-resolution orthophotos of the landslide area with a resolution of 2 cm/pix. On the developed orthophotos the body of the Celario flowslide was traced. It produced a scar in the vegetation and destroyed and damaged several buildings with a total length of 1510 m and a relief energy of 608 m. The flowslide was triggered by the failure of a shallow soil cover less than 1 m thick located at 703 m a.s.l. This first trigger is a soil failure developed from a tuff ridge, which successively impacted the downslope soil cover (after a 60-m fall) that started the main flowslide, as shown in the frontal orthomosaic of the crown area of the Main Map.

4.2. Map 2 – Geology of the flowslide and cross-section

The geological map of the landslide was developed from both the field survey and UAV-derived orthomosaic. The outcropping lithologies were classified following the legend of formations proposed by Sbrana et al. (2018). Most of the described succession cropped out along the main pathway of the flowslide in the sliding zone, as shown in Figure 3(a).

Table 2. Maximum rainfall recorded at different durations with relative time of occurrence and daily accumulation.

Raingauge	Max 10′ (mm)/time	Max 20′ (mm)/time	Max 30′ (mm)/time	Max 1h (mm)/time	Max 3h (mm)/time	Max 6h (mm)	Max 12h (mm)	Max 24h (mm)	Daily
Forio	11.2/05:00	20.6/05:10	31.6/05:20	57.6/05:20	97.6/05:20	131.4	168.0	176.8	176.8
Ischia	12/08:20	19.4/08:30	26.8/08:40	40.6/09:00	62.8/10:00	118.6	156.0	162.4	162.4
Piano Liguori	9.8/08:40	18.4/08:40	27.4/08:40	43.6/09:00	63.4/11:00	93.4	142.8	149.8	149.8
Monte Epomeo	13.4/05:00	19.6/05:00	30/05:00	50.4/05:00	82.6/05:10	109.4	137.8	145.4	145.4

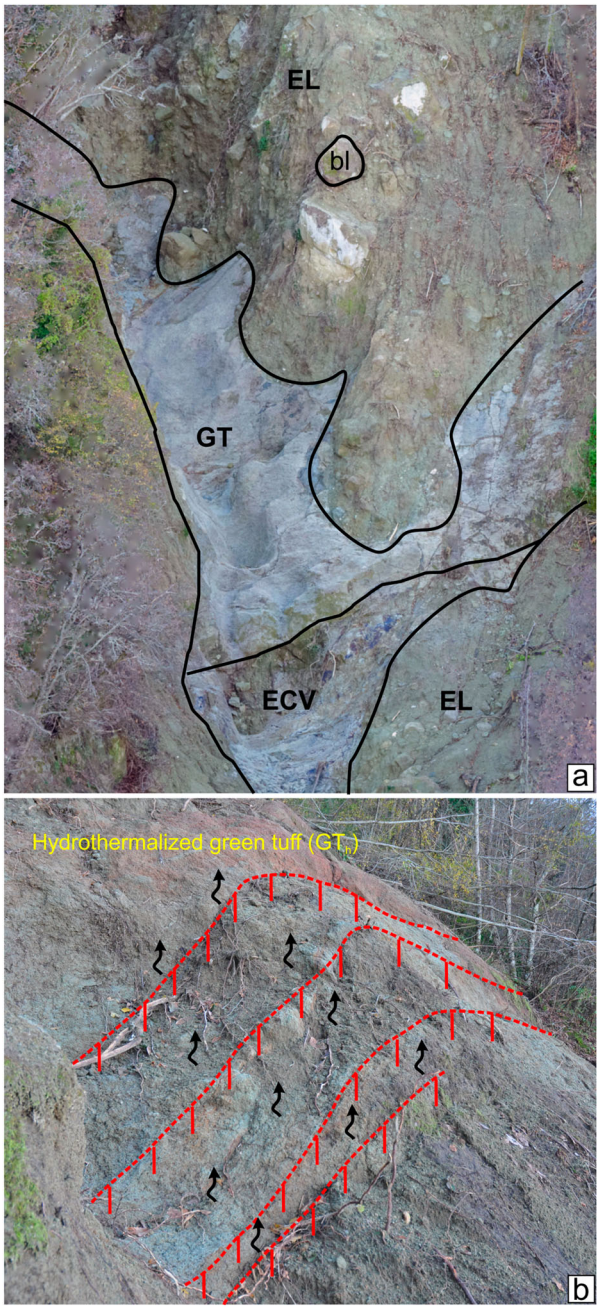

Figure 3. Frontal orthomosaic and field pictures of the sliding zone and crown area. (a) Marine deposits (ECV) to tuff (GT) stratigraphic sequence covered by the debris flow deposits (EL) and (b) sub-vertical normal faults of the Celario flowslide crown area that enable the migration of hydrothermal fluids. Black lines: formation limits; red lines: normal faults; black arrows: hydrothermalised fluids uprise.

The geological setting includes the following lithologies:

- **ECV**: Cava Celario epiclastics, silty and arenaceous marine deposits (Sbrana et al., 2018), rich in microfossils, from massive to laminated.
- **GT**: Massive, yellowish-greenish, ashy and pumice-rich welded tuffs, locally fractured and stratified and dated 62000 yr. B.P. (Sbrana et al., 2018), which represents the main bedrock unit. Several sub-vertical normal faults mainly E-W oriented can be found in the crown and sliding areas, see Figure 3(b). These volcano-tectonic features permit the upward migration of hydrothermal fluids that affect the tuff mineralogy, which is composed of oxidised and reddish minerals showing cohesive facies (**GT$_h$**).
- **EL**: Deposits of the ancient debris flows originated during the uplift phase of Mt. Epomeo aged post 6000 – present (Sbrana et al., 2018). Several tuff boulders and blocks (>2 m^3) are embedded within the **EL** deposits and clearly observable throughout the landslide (**bl**).
- **Ws**: Weathered soil cover over the bedrock made of a 30–50 cm-thick coarse sands, pumices, scoriaes and sandy silts.
- **LB**: Main deposit of the flowslide, starting at about 255 m a.s.l. with thickness up to 7–8 m. It can be divided into a proximal (**LBa**) and a distal facies (**LBb**). The former is made of coarser material also hosting transported objects and blocks (**blt**) taken from the channel, while the latter is the most liquid part of the flowslide that moved following the main roads.

Map 2 also shows the trace of the geological cross-section reported in the Main Map. It highlights the strong volcano-tectonic control on the stair-like green tuff (GT) bedrock, which is covered by variable thickness of Ws. Additionally, the topographic profile before the Celario flowslide, derived from a pre-event LiDAR, was reported in the cross-section. The whole flowslide is made of three parts characterised by different slope angle values. The crown is highly dipping (about 42°) and is located at about 645 m a.s.l. The sliding zone, dipping about 29°, represents the area where the flowslide increased its volume entraining materials from the channel. Finally, the Angle of Reach (Corominas, 1996) of the landslide, calculated as the angle of the line connecting the landslide crown height and the whole displaced mass toe, is equal to 24°.

4.3. Map 3 – Geomorphology of the flowslide

The whole flowslide involved a total area of about 70,000 m^2, where 30,000 m^2 is represented by the sliding zone on the slope and 40,000 m^2 is the deposition zone, which involves the urban area. The geomorphological map of the landslide (Map 3 in the Main Map) was obtained by observations from field and UAV surveys. It shows the three sectors of the crown, the sliding zone and the deposition area, which is identified downvalley of the fcf (first foothill change) line. Furthermore, it permitted to also highlight some lateral smaller flowslides on the left flank. On the right flanks of the deposition area, three other smaller crowns were found that originated flowslides reaching the main body.

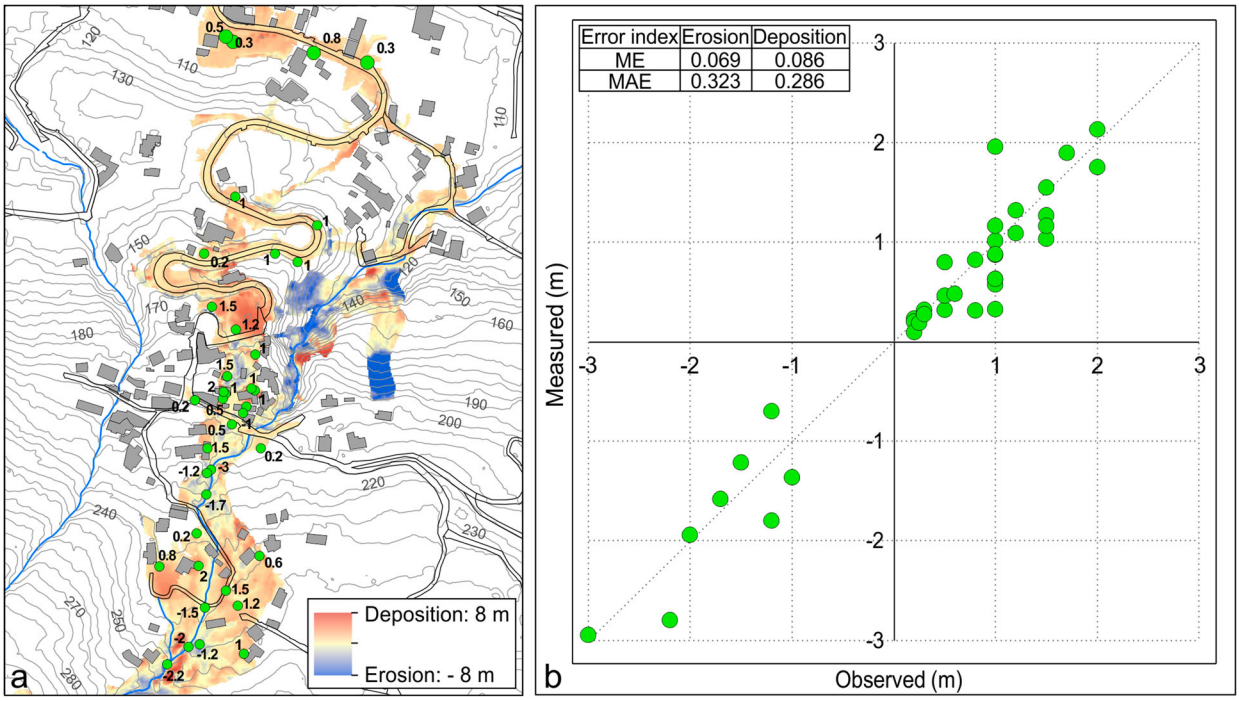

Figure 4. (a) DoD map with location of the check points surveyed in the field. (b) Comparison of the erosion and deposition values obtained between field survey (measured) and DoD (observed).

The central part of the body is characterised by a relevant run-off, which dissected the main channel and its lateral portions. The downcutting is also highlighted by several rills and gullies that are mainly located downslope of fault-related scarps in the upper portion and man-made scarps in the urban area. In the latter, the proximal facies of the event was deposited and strong modifications of the natural hydrographic network can be observed. In fact, the flowslide exposed some buried check-dams and hydraulic works that diverted the original channel highly affecting the buildings. Conversely, the distal depositional facies, where the mass became a hyper-concentrated flow, mainly moved following the roads with a high transport of objects, such as parked cars and buses.

4.4. Map 4 – DoD and transversal topographic profiles

SfM photogrammetry from UAV permitted to produce DSM and DTM of the study area. The DTM

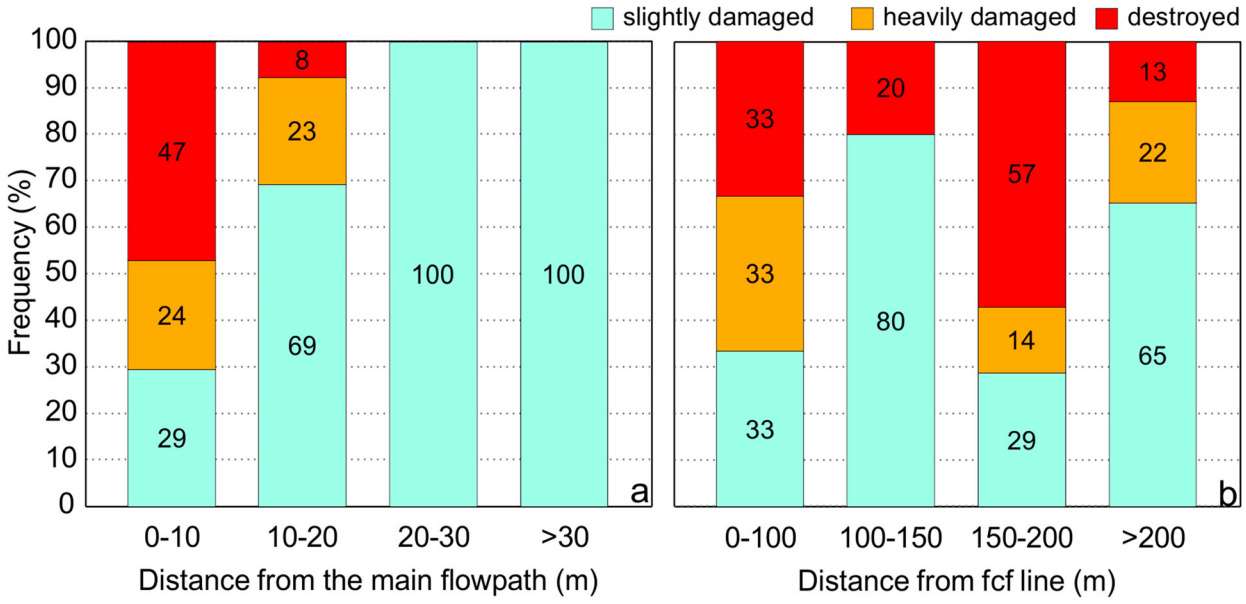

Figure 5. Influence of (a) the distance from the main flowpath and (b) distance from the 'fcf' (first slope change at foothill) line on the damaged buildings.

was subtracted from pre-landslide LiDAR-derived DEM to produce the DEM of Difference (DoD) reported in Map 4. It is a widely adopted tool concerning volumetric Geomorphic Change Detection that could reveal the main areas of erosion and accumulation (Bull et al., 2010; DeLong et al., 2012; Jaboyedoff et al., 2012). The erosion and deposition thickness values are shown in a ±8 m range, with the warm colours indicating deposition and the cold colours indicating erosion. This map highlights the erosion areas represented by the secondary crowns as well as the main channel, while the accumulation of the landslide deposits occurs with maximum thickness values in the urban area after the fcf line.

In Figure 4(a), the location of field observations used to validate the DoD is reported, some examples are also reported in Pictures 1–4 of the Main Map. They show a mean value of 0.5 m of erosion in the triggering area (Map 4 P1) and on the flanks (Map 4 P2), while erosion values as high as 7–8 m are in the main channel of the sliding area (Map 4 P3). As regards the deposition values, they are less representative of the occurred phenomena, as rescue operations moved and displaced the mud. In Map 4 P4, an example of the flowslide accumulation is reported. Figure 4(b) shows the comparison between field-measured data with those obtained from DoD. Mean Error (ME) and Mean Absolute Error (MAE) were estimated, both showing very low values.

Finally, Map 4 was also adopted to trace transversal topographic profiles, they were aimed at comparing the mobilised thickness for different sectors of the landslide. This analysis permitted to estimate the whole volume and to highlight the presence of channels where major erosion occurred. The estimated volumes are around 50,000 m^3, in agreement with Romeo et al. (2023) who found about 40,000 m^3.

4.5. Map 5 – Building damage

The Map 5 in the Main Map reports the building damage, which provides a qualitative description of the impact of the Celario flowslide in the urban area. The buildings were classified as 'unaffected', 'shifted', 'slightly damaged', 'heavily damaged', or 'destroyed' based on observations from field-acquired pictures (P5-13). The 'slightly damaged buildings' are those invaded by the mud and show minor structural damages (P5, 7). The 'heavily damaged buildings' showed major structural damages (P10, 11), while the 'shifted' buildings were completely displaced by the flowslide (P9). The footprints of the buildings before the events were obtained from the regional cartography and pre-landslide LiDAR-derived DSM. The 'destroyed buildings' were partly or completely destroyed by the Celario landslide (P6, 8, 12). In the distal area, where the liquid part of the flowslide moved along the road network, no remarkable damages were found (P13). A total of 11 destroyed buildings, 5 heavily damaged buildings, 28 slightly damaged buildings and 3 shifted buildings were identified.

Furthermore, the assigned damage class was compared with the distance from the main flowpath and the first slope change at the foothill (fcf) in Figure 5. In Figure 5(a), the nearest class of distance (0–10 m) displays the highest (about 45%) percentage of destroyed buildings, while the heavily damage (about 25%) and the slightly damaged (about 30%) show lower values. In the 10–20 m, the percentage of slightly damaged buildings increases (about 70%), while the percentage of destroyed buildings decreased to about 10%. On the other hand, further than 20 m there are only slightly damaged buildings. Therefore, the severity of the damage reduces with increased distance from the main flowpath.

As regards the distance from fcf line in Figure 5(b), the level of damage varies less regularly. The highest percentage of destroyed buildings is observed in the 150–200 m (about 60%), while the lowest (about 15%) in the >200 m class. The 100–150 m and the >200 m classes show high percentages of slightly damaged buildings (80% and 65%, respectively), whereas in the 0-100 m and in the 150–200 m classes they are 33% and 29%, respectively.

5. Discussion and conclusions

The rainfall event that occurred on the night of 26th November 2022 on Ischia Island triggered several landslides as well as a flood. The most affected municipality was Casamicciola, where the Celario flowslide occurred. It was characterised by a first failure of the soil cover at the top of Mt. Epomeo, whose downslope impact triggered the main slide. The latter flew along the pre-existing channel impacting the urban area with relevant damage to the buildings and causing many casualties. The more fluid part of the event continued its path for over 500 m along a channel-road, which was completely flooded for a height of about 1 m and where many cars were dragged.

Post-event field surveys as well as 3D models derived from UAV-acquired images allowed the mapping of the occurred phenomena. In particular, the geological and the geomorphological maps were produced, while the elaboration of the Dem of Difference (DoD) permitted to have a user-friendly tool for the distribution and quantification of the amount of eroded and deposited material. The latter was estimated to be around 50,000 m^3. As regards the building damage, it was found that those closer to the main flowpath registered the highest levels of damage, which decreases with increasing distances. Conversely,

no regular relationship between damage and distance from the foothill was observed. However, on the flanks and in the distal area lower damage occurred.

In conclusion, this study can provide a methodological example for the reconstruction of the phenomenon immediately after the event. Furthermore, the perimeter of the flowslide, as well as the estimate of the mobilised material can be used in the modelling of flow propagation. The latter will permit to draw possible scenarios for the definition of the most suitable risk mitigation strategies.

Software

The UAV images were processed with AGISOFT METASHAPE PRO® software, while the spatial analyses were performed using Esri ArcGIS 10.2. The final layout of the maps was edited using Corel Draw X7. The field pictures were localised with the software Geosetter.

Acknowledgements

The authors wish to thank the Protezione Civile for enabling the access to the locations where the surveys were conducted during the days following the landslide event. Moreover, we are grateful to the three reviewers for their useful comments and observations that helped improving the overall quality of the manuscript.

Disclosure statement

No potential conflict of interest was reported by the author (s).

Funding

The work included in this study benefited from the support of DPC ReLUIS project funded by the University of Naples (Scientific Coordinator: Prof. Antonio Santo).

Data availability statement

The rainfall data used in this study are available at http://centrofunzionale.regione.campania.it. The pre-event LiDAR is available upon request at https://sit.cittametropolitana.na.it/index.php. The other produced data will be made available by the Authors upon request.

ORCID

Luigi Massaro http://orcid.org/0000-0002-8830-1478

References

Alvioli, M., Melillo, M., Guzzetti, F., Rossi, M., Palazzi, E., von Hardenberg, J., Brunetti, M. T., & Peruccacci, S. (2018). Implications of climate change on landslide hazard in Central Italy. *Science of the Total Environment*, *630*, 1528–1543. https://doi.org/10.1016/j.scitotenv.2018.02.315

Bull, J. M., Miller, H., Gravley, D. M., Costello, D., Hikuroa, D. C. H., & Dix, J. K. (2010). Assessing debris flows using LIDAR differencing: 18 May 2005 Matata event, New Zealand. *Geomorphology*, *124*(1), 75–84. https://doi.org/10.1016/j.geomorph.2010.08.011

Chiesa, S., Civetta, L., De Lucia, M., Orsi, G., & Poli, S. (1987). Volcanological evolution of the island of Ischia. *Rend Acc Sci Fis Mat Napoli Special Issue*, 69–83.

Civetta, L., Gallo, G., & Orsi, G. (1991). Sr- and Nd-isotope and trace-element constraints on the chemical evolution of the magmatic system of Ischia (Italy) in the last 55 ka. *Journal of Volcanology and Geothermal Research*, *46*(3), 213–230. https://doi.org/10.1016/0377-0273(91)90084-D

Corominas, J. (1996). The angle of reach as a mobility index for small and large landslides. *Canadian Geotechnical Journal*, *33*(2), 260–271. https://doi.org/10.1139/t96-005

DeLong, S. B., Prentice, C. S., Hilley, G. E., & Ebert, Y. (2012). Multitemporal ALSM change detection, sediment delivery, and process mapping at an active earthflow. *Earth Surface Processes and Landforms*, *37*(3), 262–272. https://doi.org/https://doi.org/10.1002esp.2234

Del Prete, S., & Mele, R. (1999). L'Influenza dei fenomeni d'instabilita di versante nel quadro morfoevolutivo della costa dell'isola d'Ischia. *Bollettino della Società geologica italiana*, *118*(2), 339–360.

Del Prete, S., & Mele, R. (2006). Il contributo delle informazioni storiche per la valutazione della propensione al dissesto nell'Isola d'Ischia. *Rendiconti Societa Geologica Nuova Serie*, *2*, 29–47.

Gargiulo, F., Forte, G., d'Onofrio, A., Santo, A., & Silvestri, F. (2022). Seismic performance of slopes at territorial scale: The case of Ischia Island. *Proceedings of the 4th International Conference on Performance Based Design in Earthquake Geotechnical Engineering, Beijing.*

Jaboyedoff, M., Oppikofer, T., Abellán, A., Derron, M.-H., Loye, A., Metzger, R., & Pedrazzini, A. (2012). Use of LIDAR in landslide investigations: A review. *Natural Hazards*, *61*(1), 5–28. https://doi.org/10.1007/s11069-010-9634-2

Messeri, A., Morabito, M., Messeri, G., Brandani, G., Petralli, M., Natali, F., Grifoni, D., Crisci, A., Gensini, G., & Orlandini, S. (2015). Weather-related flood and landslide damage: a risk index for Italian regions. *PLoS One*, *10*(12), e0144468. doi:10.1371/journal.pone.0144468

Neumayer, E., & Barthel, F. (2011). Normalizing economic loss from natural disasters: A global analysis. *Global Environmental Change*, *21*(1), 13–24. https://doi.org/10.1016/j.gloenvcha.2010.10.004

Orsi, G., De Vita, S., & Piochi, M. (1998). The volcanic island of Ischia. *Volcanic Hazards and Risk in the Parthnopean Megacity. Int. Meeting 'Cities on Volcanoes' Rome and Naples.*

Romeo, S., D'Angiò, D., Fraccica, A., Licata, V., Vitale, V., Chiessi, V., Amanti, M., & Bonasera, M. (2023). Investigation and preliminary assessment of the Casamicciola landslide in the island of Ischia (Italy) on November 26, 2022. *Landslides*, *20*, 1265–1276. https://doi.org/10.1007/s10346-023-02064-0

Salvati, P., Pernice, U., Bianchi, C., Marchesini, I., Fiorucci, F., & Guzzetti, F. (2016). Communication strategies to address geohydrological risks: the POLARIS web initiative in Italy. *Natural Hazards and Earth System Sciences*, *16*(6), 1487–1497. doi:10.5194/nhess-16-1487-2016

Santangelo, N., Forte, G., De Falco, M., Chirico, G. B., & Santo, A. (2021). New insights on rainfall triggering flow-like landslides and flash floods in Campania (Southern Italy). *Landslides*, *18*(8), 2923–2933. https://doi.org/10.1007/s10346-021-01667-9

Santo, A., Di Crescenzo, G., Del Prete, S., & Di Iorio, L. (2012). The Ischia island flash flood of November 2009 (Italy): Phenomenon analysis and flood hazard. *Physics and Chemistry of the Earth, Parts A/B/C*, *49*, 3–17. https://doi.org/10.1016/j.pce.2011.12.004

Sbrana, A., Marianelli, P., & Pasquini, G. (2018). Volcanology of Ischia (Italy). *Journal of Maps*, *14*(2), 494–503. https://doi.org/10.1080/17445647.2018.1498811

Selva, J., Acocella, V., Bisson, M., Caliro, S., Costa, A., Della Seta, M., De Martino, P., de Vita, S., Federico, C., Giordano, G., Martino, S., & Cardaci, C. (2019). Multiple natural hazards at volcanic islands: a review for the Ischia volcano (Italy). *Journal of Applied Volcanology*, *8*(1), 5. https://doi.org/10.1186/s13617-019-0086-4